

# Conceptual foundations

---

This chapter reviews the essential conceptual backgrounds for the different spectroscopic analyses and theoretical calculations.

## 3.1. Photophysical pathways of electronic energy dissipation

Absorption of visible and ultra-violet radiation triggers transitions between electronic states and therefore can be recorded as a trace of the absorbance as the frequency varies, which is called an absorption spectrum. A given sample continues to show an absorption spectrum for as long as the irradiation source is present, which means that a finite number of sample molecules are apparently capable of absorbing infinite amount of energy. But actually an electronically excited molecule gets rid of the absorbed energy, after doing some photophysical activity or participates in a photochemical reaction and loses its identity<sup>3,4</sup>.

In monatomic gases at low pressure and temperature, the reverse transition with emission is the most probable way to lose the excitation energy. However, in condensed systems, e.g. solutions, liquids, solids, polyatomic molecules and gases at moderate pressures, there are multiple pathways available for the dissipation of the excitation energy of an electronically excited molecule. The priorities of these pathways are established by their relative rate constants, and to be competitive all these photophysical processes must occur in a time period faster than the natural radiative lifetime of the molecule. Among the various possible photophysical processes, some are intrinsic properties of the molecule and are unimolecular in nature, whereas some others depend on external perturbations and may require bimolecular collisions. A complete understanding of the photochemical and photophysical processes ensuing photoexcitation is essential to assess how the absorbed quantum of energy is partitioned into different pathways. This account keeping is required if a chemical reaction is needed to be modified<sup>7,30</sup>.

### 3.1.1. Unimolecular processes of energy dissipation

The unimolecular processes are better represented pictorially using the Jabłoński diagram<sup>4, 30, 121</sup> as shown in figure 3.1. It illustrates the electronic states of a molecule and the transitions between them through a schematic diagram, where the states are arranged vertically by energy

and grouped horizontally by spin multiplicity. Jabłoński diagram ignores the finely spaced rotational levels but each electronic level is shown to be associated with closely spaced vibrational levels. In the common descriptions, the molecule is assumed to remain in singlet ground state. Nonradiative transitions are indicated by curvy arrows and radiative transitions by straight arrows.

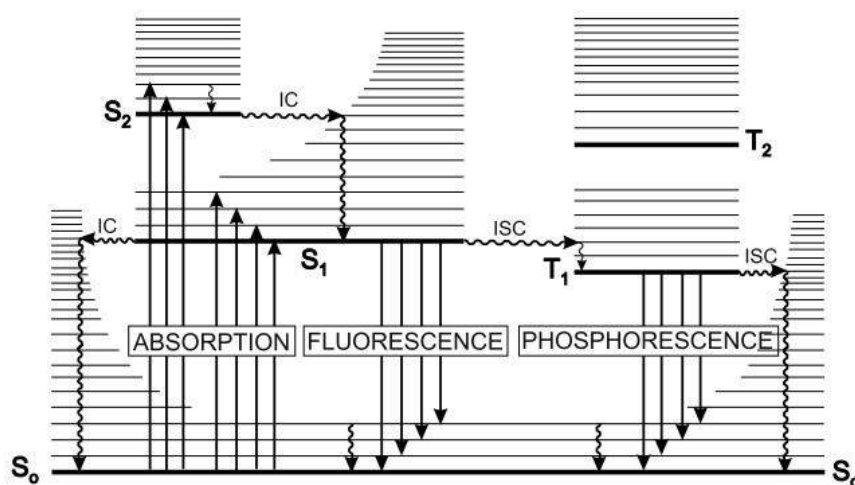


**Figure 3.1.** The Jabłoński diagram<sup>30</sup>.

The initial act of absorption instantly ( $\sim 10^{-15}$  s) photoexcites a molecule, in its ground singlet state S<sub>0</sub>, to a higher vibrational level of the first excited state S<sub>1</sub> or to an energy state higher than S<sub>1</sub>, according to the Frank-Condon principle. With a few rare exceptions, molecules in condensed phases lose their excess electronic and vibrational energy rapidly ( $\sim 10^{-13} - 10^{-11}$  s) to the surroundings and reaches the zero vibrational level of the first excited singlet state S<sub>1</sub>. This radiationless cascade of energy is known as internal conversion (IC). Once in the zero vibrational level of S<sub>1</sub>, the molecule reverts back to the ground state S<sub>0</sub>, by nonradiative internal conversion, or by radiative fluorescence emission, or by a combination of nonradiative and radiative pathways in accordance to the Kasha's rule<sup>7,8</sup>. The internal conversion (IC) process from S<sub>1</sub> to S<sub>0</sub> is slower ( $\sim 10^{-8} - 10^{-7}$  s) than the same processes in higher energy states owing to the large energy gap between S<sub>1</sub> and S<sub>0</sub>. The radiative fluorescence emission has a rate constant of about  $10^9$  s<sup>-1</sup> and it also follows the Frank-Condon principle. The third possibility is the nonradiative transition from singlet to nearby triplet state through the cross-over point of the two potential energy curves in a process known as intersystem crossing (ISC). Although the  $\Delta S=0$  rule forbids

spectroscopic transitions between singlet and triplet, such transitions can take place kinetically through radiationless transitions induced by collisions in a short time scale ( $\sim 10^{11} - 10^9 \text{ s}^{-1}$ )<sup>3</sup>.

Once the molecule reaches the triplet state, it loses its excess electronic and vibrational energy swiftly as internal conversion (IC), and arrives at the zero vibrational level of the lowest energy triplet state  $T_1$ . From the lowest vibrational level of  $T_1$  the molecule can make another nonradiative transition to the ground state  $S_0$ . That is also an intersystem crossing (ISC) process, but occasionally called the reverse intersystem crossing process<sup>4</sup>. The molecule can also de-excite by making a forbidden spectroscopic transition to  $S_0$  and by emitting phosphorescence but that process is much slower than an allowed transition. A phosphorescent material will continue to emit radiation seconds, minutes and even hours after the initial absorption<sup>3</sup>. It is also possible for the molecule in the zero vibrational level of  $T_1$  to excite to the higher vibrational levels with the aid of thermal energy, and then cross back to the  $S_1$  state through the isoenergetic point via intersystem crossing<sup>4</sup>. The molecule in the first excited singlet state then relaxes to the ground singlet state by emitting fluorescence emission. This type of fluorescence emission is much slower, and is known as the E-type delayed fluorescence<sup>4, 7, 30</sup>. There is another type of delayed fluorescence known as the P-type delayed fluorescence. Here, two triplet molecules encounter to give rise to an intermediate species X, which later decomposes into an excited and a ground state singlet molecule<sup>4</sup>. The excited singlet molecule loses its excitation energy finally as the radiative emission of fluorescence. Due to the possibility of these two types of delayed fluorescence, the short-lived direct fluorescence is sometimes referred to as prompt fluorescence<sup>4</sup>.

This is worthy to mention here that under special conditions, a molecule in  $T_1$  state may be photoexcited to upper triplet states  $T_n$  by absorbing suitable radiation. Since the  $T_1$  state is not stable like the  $S_0$  state, such absorption is called transient absorption<sup>26</sup>.

An important fact regarding the radiationless processes like internal conversion or intersystem crossing is that these are the intrinsic property of polyatomic molecules. Polyatomic molecules with  $(3N-6)$  or  $(3N-5)$  modes of vibrations can undergo such loss in energy even in the vapor phase at very low pressures where collision frequencies are less than the rates for radiationless conversion. In these processes, the environment acts as a heat sink for dissipation of excess energy as thermal energy<sup>4</sup>.

The selection rules for nonradiative transitions are different than those for radiative transitions. Therefore,  $S_1$  to  $T_1$  transition is allowed nonradiatively but similar transition for  $S_1$  to  $S_0$  and  $T_1$  to  $S_0$  is not allowed. These selection rules control the relative rate constants for the nonradiative transitions <sup>4</sup>.

### 3.1.2. Bimolecular processes of energy dissipation

Bimolecular processes that affect the population of the excited state could be aided by molecular collisions or by long-range dipole-dipole interactions. However, in general, any similar processes can be called the dynamic quenching. The dynamic quenching of a molecule can be further classified as the self-quenching, solvent quenching and the impurity quenching <sup>4,7</sup>.

1. Self-quenching occurs due to interactions between chromophoric molecules of the same kind, and it brings non-linearity in the relationship between fluorescence intensity and concentration. For this reason, fluorescence measurements are usually carried out at low concentration of the fluorophore.
2. Solvent quenching occurs due to collisions with the solvent molecules but such type of quenching is often classified under unimolecular processes as a clear distinction between it and the internal conversion from  $S_1$  to  $S_0$ .
3. Impurity quenching is brought about by any added foreign molecules in the system that can interact with the chromophore.

There are numerous causes for the occurrence of dynamic quenching <sup>7,30</sup>.

- Collision quenching requires the quencher to diffuse to the fluorophore during the lifetime of the excited state. Upon contact, the fluorophore returns to the ground state without emission of a photon.
- In radiative energy transfer, the photon emitted by the fluorophore is absorbed by the quencher.
- In nonradiative energy transfer, the fluorophore loses its energy to the quencher nonradiatively as a result of short- or long-range interactions.
- Photoinduced electron transfer (PET) requires the fluorophore to act as an electron donor or acceptor with the quencher acting as the acceptor or donor, respectively.

- If the contact ion pair (CIP) formed during the PET process decomposes slower than the decay time of the fluorophore, then it will be termed as an exciplex. Exciplex emission is red shifted to the fluorophore emission and it is bit delayed.
- Excimer formation results from the collision between an excited fluorophore and an identical unexcited molecule. It is also red shifted to the fluorophore emission and delayed.
- In photoinduced proton transfer (PPT), the fluorophore undergoes an acid-base reaction with the quencher and forms an electronically excited protonated or deprotonated form.

### 3.2. Characteristics of fluorescence emission

Fluorescence is an outcome of energy dissipation by electronically excited molecules and its representation as a trace of fluorescence intensity with variable frequency is called a fluorescence spectrum or emission spectrum. Fluorescence intensity is an empirical expression of fluorescence activity unlike absorbance and commonly expressed in terms of arbitrary units proportional to detector response<sup>7,8</sup>.

#### 3.2.1. Mirror image relationship

In absence of collisional perturbations at very low pressures, electronically excited atoms or molecules may return to the ground state directly by emitting the same frequency of radiation as it has absorbed. Such a radiation, known as resonance radiation, is observed for mercury at 253.8 nm. For polyatomic molecules and molecules in condensed systems, fluorescence radiation occurs due to transition from the zero vibrational state of the first excited singlet state  $S_1$  to a higher vibrational level of the ground singlet state  $S_0$ , which then quickly reaches thermal equilibrium. In most cases,  $0 \rightarrow 0$  is the most probable vibrational transition associated with the reverse transition of electron. However, often there is a distribution of frequencies around the most probable transition which depends on the nature of wave function in  $v = 0$  state in  $S_1$ , and also on the Boltzmann distribution of energy in the excited state. It is to be noted that whereas the profile of absorption spectra depends on the spacing between the vibrational bands in the excited singlet state, the fluorescence spectral profile correspond to the vibrational energy differences in the ground state. In many polyatomic molecules, internuclear geometries remain similar in both ground and excited electronic states, and as a result the fluorescence spectrum

appears as a mirror image of the corresponding absorption spectrum with a region of overlap. Mirror image relationship is not observed for small unconjugated molecules where the excited state has very different geometry from that of the ground state <sup>4,7,122</sup>.

### 3.2.2 Stokes shift

The fluorescence spectrum typically observed on the red side of the absorption spectrum. This phenomenon was first observed by Sir. G. G. Stokes in 1952 and thereafter such a shift came to be known as the Stokes shift <sup>7,8,123</sup>. The explanation can easily be sorted out using the Jabłoński diagram, which tells that due to the working of Frank-Condon principle and thermal relaxation of the vibrational modes, the emitted quanta of fluorescence are of lower energy than the absorbed quanta.

### 3.2.3. Kasha's rule

Another important characteristic of fluorescence is that the fluorescence spectrum remains the same irrespective of the excitation wavelength, only the intensities vary. Different wavelength of excitation can promote the molecule to a different higher vibrational level of  $S_1$  or to an energy state higher than  $S_1$  but nevertheless, fluorescence emission occurs in appreciable yield only from the zero vibrational level of  $S_1$ , in consequence of the Kasha's rule <sup>7,8,124</sup>, which states that photon emission, fluorescence or phosphorescence, occurs in appreciable yield only from the lowest excited state of a given multiplicity. The fluorescence intensities are altered because with different excitation wavelength, the probability of absorption varies too. The variations in fluorescence intensity as a function of the excitation wavelength for a fixed observation wavelength, in the fluorescence spectrum, represent the excitation spectrum. For a pure sample, the absorption spectral profile resembles the excitation spectral profile.

### 3.2.4. Fluorescence quantum yield

Fluorescence quantum yield is one of the most important characteristic of fluorescence emission by a molecule. A molecule with higher quantum yield displays brighter emission <sup>4,7</sup>. According to the definition of quantum efficiency of a photochemical or photophysical process, the fluorescence quantum yield is defined as the ratio of the number of photons emitted to the number absorbed. In absence of photochemical reactions, fluorescence competes with other

nonradiative pathways for the utilization of the absorbed quanta, which have been depicted in the Jabłoński diagram. If  $k_{nr}$  denotes the rate of nonradiative decay to  $S_0$  from  $S_1$  and  $k_r$  is the radiative decay rate, the fluorescence quantum yield  $\Phi_F$  is given by equation 3.1,

$$\Phi_F = \frac{k_r}{k_r + k_{nr}} \quad (3.1).$$

Quantum yield approaches unity when the nonradiative decay rates diminish to zero.

### 3.2.5. Fluorescence lifetime

Fluorescence lifetime is another most important characteristic of a fluorophore<sup>7, 30</sup>. It specifies the average time the fluorophore remains in the excited state prior to return to the ground state and determines the time available for the fluorophore to interact with or diffuse in its environment. Fluorophores with higher lifetimes acquire more information about the environment. If a fluorophore loses its excitation energy through fluorescence emission as well as through nonradiative pathways, its lifetime is given by,

$$\tau = \frac{1}{k_r + k_{nr}} \quad (3.2).$$

So, combining equations 3.1 and 3.2, the radiative and nonradiative decay rates are obtained as equations 3.3 and 3.4 respectively:

$$k_r = \frac{\Phi_F}{\tau} \quad (3.3),$$

$$k_{nr} = \frac{(1 - \Phi_F)}{\tau} \quad (3.4).$$

In absence of nonradiative processes, the lifetime of the fluorophore is called the natural lifetime and is given by equation 3.5:

$$\tau_n = \frac{1}{k_r} \quad (3.5).$$

Therefore, with the help of equations 3.3 and 3.5, the natural lifetime of the fluorophore can be calculated from the measured lifetime and the quantum yield, as in equation 3.6.

$$\tau_n = \frac{\tau}{\Phi_F} \quad (3.6).$$

Relative values of the rate constants  $k_{nr}$  and  $k_r$  determine the quantum yield and lifetime of a fluorophore. A molecule may be nonfluorescent as a result of large nonradiative decay rate or a slow rate of fluorescence emission. Molecules with higher rate of fluorescence emission have large quantum yield and shorter lifetimes.

### 3.2.6. Steady-state and time-resolved fluorescence measurements

Generally, there are two types of fluorescence measurements: steady-state and time-resolved<sup>7,31</sup>. In steady-state experiments, the sample is illuminated with a continuous beam of light and the fluorescence intensity or emission spectrum is recorded. Because of the nanosecond time scale of fluorescence, steady state is reached almost immediately after sample excitation and hence, most measurements are steady-state measurements. In time-resolved measurements the sample is exposed to a light pulse, whose pulse width is typically shorter than the decay time of the sample, and the intensity decay is recorded with a high-speed detection system. Intensity decays and anisotropy decays are measured on the nanosecond time scale using the time-resolved measurements. A steady-state observation is actually an average of the time-resolved phenomenon over the intensity decay of the sample. If a fluorophore displays a single decay time ( $\tau$ ) and a single rotational correlation time ( $\theta$ ), the intensity and anisotropy decays are given by equations 3.7 and 3.8 respectively.

$$I(t) = I_0 e^{-t/\tau} \quad (3.7),$$

$$r(t) = r_0 e^{-t/\theta} \quad (3.8),$$

Where  $I_0$  and  $r_0$  are the intensities and anisotropies at  $t = 0$ , immediately after the pulse excitation, respectively.

### 3.2.7. Inner filter effects

It is worthy to recognize that fluorescence yields are proportional to the concentration only over a limited range of absorbances and that the apparent fluorescence intensity and spectral distribution may change depending on the sample absorbance or turbidity. This is due to a phenomenon known as inner filter effect<sup>7, 8, 30</sup>. So, it is preferable to use very dilute solutions wherever possible.

If a sample has appreciable absorbance at both the excitation and emission wavelengths, the fluorescence can attenuate due to absorption of both the incident light (primary inner filter effect or excitation inner filter effect) as well as the emitted light (secondary inner filter effect or emission inner filter effect). Presence of the other chromophores in the solution that absorb light in the same wavelength range as the fluorescent compound under study can also contribute to the inner filter effect. Excitation inner filter effect reduces the fluorescence intensity, whereas emission inner filter effect modifies the fluorescence spectrum due to reduction donor fluorescence intensity in the region of spectral overlap. Emission inner filter is the consequence of radiative energy transfer which will be discussed later in section 3.5.

The precise geometry of sample illumination can control the inner filter effects <sup>125-127</sup>. Commonly fluorescence is observed at right-angle of the center of a centrally illuminated cuvette. There are other geometric arrangements including front-face and off-center illumination, which decrease the inner filter effects. Usually, the measured intensity is proportional to optical density only to an optical density of 0.05 for right-angle observation.

It is possible to make approximate corrections for the inner filter effects <sup>7</sup>. If a sample has absorbances  $A_{ex}$  and  $A_{em}$  at the excitation and emission wavelengths respectively, the corrected fluorescence intensity  $F_{corr}$  can be related to the observed intensity  $F_{obs}$  by equation 3.9.

$$F_{corr} = F_{obs} 10^{0.5(A_{ex} + A_{em})} \quad (3.9).$$

For analytical applications, when a linear relationship between fluorescence intensity and concentration is desired, a calibration curve must be prepared using the particular compounds and conditions that have been used for the actual experiment.

### 3.2.8. Calculation of quantum yield

The definition of fluorescence quantum yield has already been expressed in section 3.2.4. Commonly, quantum yield of a fluorophore is estimated by comparison with standards of known quantum yield <sup>7</sup>. Different standards are used according to the region of excitation but a particular standard can be used wherever they have appreciable absorption. A fluorescence standard should ideally have the following criteria <sup>30</sup>:

- The compound should have high fluorescence quantum yield.

- It should be available in highly pure form.
- The compound should be photochemically stable in the solid, liquid state or in solution.
- Its fluorescence spectrum and quantum yield should be independent of the excitation wavelength.
- Small overlap between absorption and fluorescence spectra of the compound for avoiding self-absorption errors.
- The absorption and fluorescence spectra of the compound should be broad, without any sharp spectral features, to avoid bandpass errors.
- The fluorescence emission of the compound should be unpolarized.

To calculate the quantum yield of a sample ( $\Phi$ ) with reference to a standard ( $\Phi_R$ ), both are excited at the same wavelength. Absorbance at the excitation wavelength, denoted by  $A$  and  $A_R$  for the sample and the reference respectively are kept below 0.05 to avoid inner filter effects. Quantum yield is calculated by comparison of the wavelength integrated intensity of the sample ( $I$ ) to that of the standard ( $I_R$ ). So, the final intuitive expression is given by equation 3.10.

$$\Phi = \Phi_R \frac{I}{I_R} \frac{A_R}{A} \left( \frac{n}{n_R} \right)^2 \quad (3.10).$$

Here,  $(n/n_R)^2$  is a correction factor, where  $n$  and  $n_R$  denote the refractive indices of the sample and the references respectively<sup>7, 125</sup>.

### 3.2.9. Fluorophores – intrinsic and extrinsic probes

Fluorescent probes or fluorophores are central to the study of fluorescence spectroscopy<sup>7, 33, 46</sup>. Their spectral properties determine the wavelength and time resolution required of the instruments. Broadly there are two main classes of fluorophores: intrinsic and extrinsic probes.

Intrinsic fluorophores are those that occur naturally of which aromatic amino acids, flavins, coumarins are examples. Frequently, the molecules of interest are nonfluorescent (e.g. DNA, RNA) or their intrinsic fluorescence is not adequate for the desired experiment (e.g. protein). In such cases, the molecules are labelled with fluorescent extrinsic probes<sup>34, 35, 41</sup>.

Extrinsic probes can be labelled via covalent bonding or through noncovalent interactions. Labeling via covalent bonding is done in a nonspecific or specific way<sup>7</sup>. Dyes like dansyl

chloride or TRITC bind covalently to any reactive amine groups present in a protein and there are fluorescent maleimide dyes like Rhodamine Red<sup>TM</sup> C<sub>2</sub>-maleimide which offer efficient site-specific labeling of proteins via coupling to a cysteine. Labelling with a noncovalently associated dye is useful when it is weakly or nonfluorescent in water at a certain wavelength region, but fluoresces strongly when bound to the macromolecule. Examples of this kind of dyes are ANS for protein labelling, DPH for membrane labelling and EB for DNA labelling.

### 3.3. Effects on fluorescence emission

#### 3.3.1. Structural effects on fluorescence emission

Structure of a chromophore plays an important role in controlling its fluorescence emission<sup>30</sup>. Most fluorescent compounds are aromatic but a few highly unsaturated aliphatic compounds are also fluorescent. So, generally, an increase in the degrees of conjugation or the extent of the  $\pi$ -electron system causes a shift of the absorption or fluorescence spectra to longer wavelengths and to an increase in fluorescence quantum yield.

In aromatic hydrocarbons the  $\pi \rightarrow \pi^*$  transitions have the lowest energy and are characterized by high molar absorption coefficients and relatively high fluorescence quantum yields. In compounds where a heteroatom is involved in the  $\pi$ -system, an  $n \rightarrow \pi^*$  transition may be the lowest-lying transition. However, such transitions are characterized by low molar absorption coefficients and long radiative lifetime, and are the cause for low quantum yields in most azo compounds and some compounds containing carbonyl groups and nitrogen heterocycles.

A more flexible fluorophore suffers lesser number of collisions and hence has higher probability of nonradiative deactivation via internal conversion and intersystem crossing which results in low fluorescence yield.

The effect of substituents on the fluorescence characteristics of aromatic hydrocarbons is quite complex and especially difficult if more than one substituent is present. For a single substituent, the effect depends on both the nature and position of the substituent.

- The presence of heavy atoms, in general, reduces the fluorescence quantum yields, because of the increased probability of intersystem crossing. Intersystem crossing is

avored by the efficiency of spin-orbit coupling which has a  $Z^4$  dependence,  $Z$  being the atomic number of the heavy atom.

- The presence of electron-donating substituents ( $-\text{OH}$ ,  $-\text{OR}$ ,  $-\text{NH}_2$ ,  $\text{NHR}$ ,  $-\text{NR}_2$ ), typically increases the molar absorption coefficient, causes a shift in both absorption and fluorescence spectra and makes the spectra broad and often structureless.
- Presence of electron withdrawing carbonyl substituents makes the situation more complex, because of the relative energy of  $\pi \rightarrow \pi^*$  and  $n \rightarrow \pi^*$  transitions, which varies compound to compound. Compounds like benzophenone, anthrone etc. have low-lying  $n \rightarrow \pi^*$  excited state and thus exhibit low fluorescence quantum yields. Compounds like fluorenone have a reasonable quantum yield owing to a low-lying  $\pi \rightarrow \pi^*$  excited state. If the two states have low energy difference, the fluorescence quantum yield strongly depends on the solvent polarity.
- Aromatic hydrocarbons possessing an electron withdrawing  $-\text{NO}_2$  substituent are usually non-fluorescent due to the existence of low-lying  $n \rightarrow \pi^*$  transition.
- Sulfonate substituent slightly affects the fluorescence characteristics of the parent molecule. Usually, there is a small red shift of the fluorescence spectrum, slightly decreased quantum yield and somewhat blurred vibrational structure.

### 3.3.2. Effect of solvent nature on fluorophore emission - the classical approach

Classically, a solvent is considered a macroscopic continuum characterized only by its macroscopic physical constants such as boiling point, vapor pressure, density, cohesive pressure, index of refraction, relative permittivity, thermal conductivity, surface tension, etc. But in fact, a solvent is a discontinuum which consists of individual, mutually interacting solvent molecules, characterized by their molecular properties such as polarity, electronic polarizability, hydrogen-bond donor (HBD) and hydrogen-bond acceptor (HBA) capability, electron-pair donor (EPD) and electron-pair acceptor (EPA) capability, etc. Hence, the effects of solvent on fluorescence spectra are generally complex<sup>7, 128</sup>. Typically, numerous factors contribute to the solvent dependent shift of the emission spectra. Usually such solvent effects have been attempted to understand in terms of the polarity of the solvent. Solvent polarity is a commonly used term related to the capacity of a solvent for solvating dissolved charged or neutral, apolar or dipolar, species. This concept of solvent polarity is easily grasped qualitatively, but it is difficult to define

precisely and even more difficult to express quantitatively. Attempts to express it quantitatively have mainly involved physical solvent properties such as relative permittivity, dipole moment, or refractive index. The Onsager description of non-specific electrostatic solute–solvent interactions represents the general form of such approaches<sup>128, 129</sup>. However, this approach is often inadequate since it regards solvents as a non-structured isotropic continuum and also ignores the structure of the fluorophore. But each solvent is composed of individual solvent molecules with their own solvent–solvent interactions, and specific solute–solvent interactions. Specific interactions such as hydrogen bonding, formation of charge transfer states, probe-probe interactions, conformational changes, preferential solvation etc. often produce substantial spectral shifts and if not recognized, limit the detailed interpretation of the fluorescence emission spectra. Moreover, solvent dipole moments are inadequate measures of solvent polarity since the charge distribution of a solvent molecule may not only be given by its dipole moment but also by its quadrupole or higher multipole moments, leading to dipolar, quadrupolar, octupolar, etc. solvent molecules.

Preliminarily we will describe the general Onsager description of non-specific electrostatic solute–solvent interactions along with its common approximated form. Such description of solvent effects is also known as the general solvent effects. Deviations from the behavior predicted by the theory of general solvent effects indicate the presence of additional specific interactions. Supplementary experiments are often performed to investigate in detail the nature of such interactions.

In the theory of general solvent effects, the fluorophore is assumed to be a spherical dipole centered in a closed spherical first solvation shell of a continuous dielectric solvent<sup>129-131</sup>. The dipolar fluorophore is acted upon by the reactive electric field set up by the solvent molecules which is proportional to the dipole moment of the fluorophore ( $\mu$ ) and is parallel and opposite to the direction of the dipole. Moreover, the magnitude of the field is controlled by the electronic and molecular polarizability of the solvent molecules.

The electronic polarizability depends on the motion of electrons within the solvent molecules and is described by the refractive index ( $n$ ) of the solvent<sup>7</sup>. Electronic polarization is an instantaneous process and can simultaneously stabilize both the ground and the excited states to an almost equal extent. Hence, electronic redistribution contributes negligibly towards Stokes

shift of the fluorescence spectra. It is, however, worthy to mention that absorption spectra is influenced only by the electronic polarization and for this reason, most chromophores display a red shift of the absorption spectrum in solvents relative to the vapor phase.

Molecular polarizability of a solvent results from the reorientation of the solvent dipoles which involve movement of the entire solvent molecule <sup>7</sup>. So, the stabilization of ground and excited states resulting from the molecular polarization of the solvent molecules is time dependent (10-100 ps). Due to such slow rate light absorption is not influenced by dipolar reorientation. However, in fluid solvents, solvent reorganization or relaxation is complete prior to fluorescence emission and in such cases such stabilization can result in substantial Stokes shift. The theory of general solvent effects considers solvent relaxation as the only factor contributing towards Stokes shift.

The static dielectric constant ( $\epsilon$ ) of a solvent incorporates the effects of both the electronic and molecular polarizability <sup>7, 132</sup>. Hence, the effect of solvent reorientation on reactive electric field is expressed as the orientational polarizability  $f(\epsilon, n)$ , which is obtained by eliminating the effect of electronic polarization from the net polarization obtained from the dielectric constant, as expressed in equation 3.11.

$$f(\epsilon, n) = \frac{\frac{\epsilon - 1}{2\epsilon + 1} - \frac{n^2 - 1}{2n^2 + 1}}{\left(1 - \frac{2\alpha}{a^3} \cdot \frac{\epsilon - 1}{2\epsilon + 1}\right) \left(1 - \frac{2\alpha}{a^3} \cdot \frac{n^2 - 1}{2n^2 + 1}\right)^2} \quad (3.11),$$

Where,  $\alpha$  is the average polarizability ( $\alpha_e \approx \alpha_g = \alpha$ ) of the fluorophore and  $a$  is the cavity radius in which the fluorophore resides.

Lippert and Matage simplified the expression of orientational polarizability by considering the scenario presented by common fluorophore solutions <sup>133, 134</sup>. In their description, the polarizability of the fluorophore has been ignored, the higher order terms are ignored and the ground and excited states dipole moments are assumed to point in the same direction. The higher order terms would account for the second order effects, such as the dipole moments induced in the solvent molecules resulting by the excited fluorophore and vice versa <sup>7</sup>. According to them, the orientational polarizability is given by equation 3.12.

$$f_{LM}(\varepsilon, n) = \frac{\varepsilon - 1}{2\varepsilon + 1} - \frac{n^2 - 1}{2n^2 + 1} \quad (3.12),$$

The Stokes shift is expressed as a function of the orientational polarizability and the difference between the dipole moment of the fluorophore in ground and excited states.

$$\sigma_A - \sigma_F = \frac{2(\mu_E - \mu_G)^2}{hca^3} f_{LM}(\varepsilon, n) + \text{const} \quad (3.13),$$

$$\sigma_A - \sigma_F = mf_{LM}(\varepsilon, n) + \text{const} \quad (3.14),$$

where,

$$m = \frac{2(\mu_E - \mu_G)^2}{hca^3} \quad (3.15).$$

Hence, the difference between the ground and excited state dipole moments are given by equation 3.16.

$$\Delta\mu = (\mu_E - \mu_G) = \left( \frac{1}{2} hca^3 \cdot m \right)^{\frac{1}{2}} \quad (3.16).$$

### 3.3.3. Empirical Parameters of Solvent Polarity

It has been mentioned already that a more general definition of solvent polarity would be useful for the general understanding of solvent induced spectral shifts. The most pragmatic definition has been put forward by Christian Reichardt in 1965 and later included in the ‘‘IUPAC Recommendations 1994’’. It states that the polarity of a solvent is determined by its solvation capability (or solvation power) for solutes in their ground and excited states. It embraces the action of all possible, specific and nonspecific, intermolecular forces between solute ions or molecules and solvent molecules, excluding such interactions leading to definite chemical alterations of the ions or molecules of the solute. These intermolecular forces include Coulomb interactions between ions, directional interactions between dipoles, inductive, dispersion, hydrogen-bonding, and charge-transfer forces, as well as solvophobic interactions. Protonation, oxidation, reduction, complex formation, or other chemical processes are not considered<sup>128, 135</sup>.

Obviously, no single macroscopic physical parameters could possibly account for the multitude of complex solute-solvent interactions on the molecular-microscopic level. This also prevents the

derivation of generally applicable mathematical expression for the quantification of solvent dependent processes. Such a situation has stimulated attempts to introduce empirical scales of solvent polarity<sup>128, 136, 137</sup>. The common approach has been to select a convenient, well-known, sufficiently solvent-sensitive reference process which should reflect all possible solute-solvent interactions. This reference process can be considered as a suitable model for a large class of related solvent-induced processes and a probe of the solvation shell of the standard solute. Spectral absorption and emission of a highly solvatochromic chromophore often serves this purpose and helps to provide an empirical measure of solvation capability of any particular solvent. The “empirical treatment” of solvent polarity has been a huge success to reflect the complete picture of all intermolecular forces acting in solution. Therefore, quite a few such empirical solvent scales have been developed over the years which constitute a more comprehensive measure of solvent polarity than any other single physical constant. According to Abboud and Notario, the success is frequently assisted by the regularities displayed in many cases by solvent effects<sup>136</sup>. However, the application of these solvent polarity parameters is valid only for closely related solvent-sensitive processes and is not expected to be universal and useful for all kinds of processes.

#### 3.3.4. Z parameter of solvent polarity

Historically, Grunwald and Winstein were the forerunners in the development of empirical scales of solvent polarity, who in 1948 established a linear free energy relationship between relative rate constants and the ionizing power of various solvent systems, describing the effect of solvent as nucleophile on different substrates. That relationship defines the Grunwald-Winstein parameter  $Y$ <sup>138</sup>.

Brooker *et.al.* in 1951 was the first to suggest that solvatochromic dyes should be used as indicators of solvent polarity<sup>139</sup>, but Kosower in 1958 was the first to set up a comprehensive solvent scale, the Z scale of solvent polarity<sup>140-142</sup>. He took 1-ethyl-4-(methoxycarbonyl)pyridinium iodide as the standard solute. The longest wavelength intermolecular charge transfer (CT) transition of the chromophore is highly solvent sensitive. A solvent change from pyridine to methanol causes a hypsochromic shift of the CT band of  $\Delta\lambda = -88$  nm. He described his polarity parameter, Z, as the molar transition energy,  $E_T$ , expressed in Kcal/mol for the CT absorption band of the compound in the appropriate solvent. A Z value of

83.6 for methanol means that transition energy of 83.6 kcal is necessary to photoexcite one mole of methanolic solution of the standard dye, from its electronic ground state to its first excited state. A high  $Z$  value corresponds to high solvent polarity.  $Z$  values cover a range from 94.6 (water) to about 60 Kcal/mol (i-octane).  $Z$  values have been measured for a large number of pure solvents and binary solvent mixtures. Relationships of the available  $Z$  values with other solvent polarity scales have also been compiled.

No correlation was observed between  $Z$  values and the relative permittivity or its functions. For practical purposes  $Z$  values have been widely used to correlate other solvent-sensitive processes with solvent polarity, e.g. the  $n \rightarrow \pi^*$ ,  $\pi \rightarrow \pi^*$ ,  $n \rightarrow \sigma^*$  absorption of various organic molecules, as well as many kinetic data<sup>128</sup>.

$Z$  values are both temperature- and pressure-dependent<sup>128</sup>. The CT absorption band is shifted towards blue as the temperature of the solution is decreased. Thus,  $Z$  values decrease with increasing temperature due to a lowering of the solute/solvent interactions at the higher temperature. Furthermore, the CT absorption band is red shifted for solutions in methanol and ethanol with increasing pressure, while for other solvents such as acetone and N,N-dimethylformamide it is shifted hypsochromically.

$Z$  values, however, cannot be measured precisely in highly polar solvents because the long-wavelength charge-transfer band moves to such short wavelengths that it cannot be observed underneath the much stronger  $\pi \rightarrow \pi^*$  absorption band of the pyridinium ion. Therefore, the  $Z$  value for water was obtained by extrapolating the  $Z$  values measured for acetone/water, ethanol/water, and methanol/water mixtures to zero organic component in a plot against Grunwald-Winstein parameter  $Y$ . Moreover, the standard pyridinium iodide is not soluble in many nonpolar solvents. By using the more soluble 4-(*t*-butoxycarbonyl)-1-ethylpyridinium iodide and pyridine-1-oxide as secondary standards, it was possible to calculate  $Z$  values of nonpolar solvents<sup>128, 137</sup>.

### 3.3.5. $E_T(30)$ parameter of solvent polarity

The most popular solvent polarity parameter  $E_T(30)$  has been proposed by Dimroth and Reichardt in 1963, based on the transition energy for the longest-wavelength solvatochromic absorption band of pyridinium N-phenolate betaine dye (dye number 30 in reference 143)<sup>128, 137</sup>,

<sup>143</sup>. The major advantage of this dye is the extraordinarily large range for the solvatochromic behavior: A solvent change from diphenyl ether to water causes a hypsochromic shift of the CT band from 810 nm to 453 nm and a change in  $E_T(30)$  value from 35.3 Kcal/mol to 63.1 Kcal/mol. So, the  $E_T(30)$  values provide a very sensitive characterization of the solvent polarity, high  $E_T(30)$  values corresponding to high solvent polarity.  $E_T(30)$  values have been determined for more than 360 pure solvents and for a great number of binary solvent mixtures.  $E_T(30)$  values are also known for some binary mixtures with limited miscibility, some ternary solvent mixtures and some room-temperature ionic liquids. A collection of  $E_T(30)$  values in pure solvents represents the most comprehensive empirical polarity scale so far known.

It is evident from the structure of the standard betaine dye that it has a localized negative charge at the phenolic oxygen atom, whereas the positive charge of the pyridinium moiety is delocalized. Therefore, in addition to the nonspecific dye-solvent interactions, the betaine dye (44) predominately measures the specific HBD and Lewis acidity of organic solvents although do not register their HBA and the Lewis basicity. It has been reported that the  $E_T(30)$  values of non-HBD solvents are influenced predominantly by the solvent dielectric constants <sup>137</sup>.

The  $E_T(30)$  values of binary solvent mixtures change monotonously, but not always linearly with mole fraction of one solvent component <sup>128</sup>. Most binary mixtures behave as more or less non-ideal solvent mixtures. Addition of a small amount of a polar solvent corresponds to an excessively large increase in  $E_T(30)$  owing to the strong preferential or selective solvation of the dipolar betaine dye by the more polar component of the binary solvent mixture. In these cases, the  $E_T(30)$  values actually measure the micropolarity of the solvation shell on the molecular-microscopic level rather than the polarity of the bulk solvent mixture.

The strong dependence of  $E_T(30)$  values on the composition of binary solvent mixtures with different polarity can be used for the quantitative determination of water in organic solvents using absorption or fluorescence spectroscopy. The  $E_T(30)$  parameter is also frequently used to report the polarity of micellar systems, microemulsions, phospholipid bilayers, model liquid membranes, polymers, organic-inorganic polymer hybrids, sol-gel matrices, surface polarities, and the retention behavior in reversed-phase liquid chromatography <sup>128</sup>. It is also used to correlate various other solvent-sensitive processes such as light absorption, reaction rates, and chemical equilibria.

Like the  $Z$  parameter, the  $E_T(30)$  parameter is also dependent on temperature and pressure<sup>136, 137</sup>. The temperature dependence is due to the thermo-solvatochromism behavior of the standard betaine dye (44) which stems from the increased stabilization of the dipolar electronic ground state of (44) relative to the less dipolar excited state with decreasing temperature, due to better solute/solvent interactions at low temperature. It can be stated that, the lower the temperature, the higher the  $E_T(30)$  value. Similarly the pressure dependence of  $E_T(30)$  is due to the piezo-solvatochromism of the betaine dye arising from better solute/solvent interactions with increasing pressure. It can be stated that, the higher the pressure, the more polar the solvent, and the higher the  $E_T(30)$  value. The temperature and pressure effects on  $E_T(30)$  further indicates its extreme sensitivity to small changes in the environment.

The primary standard betaine dye (44) is sparingly soluble in water and less polar solvents and insoluble in nonpolar solvents such as aliphatic hydrocarbons<sup>128</sup>. To overcome such problems the more lipophilic penta-*t*-butyl-substituted or penta(trifluoromethyl)-substituted betaine dyes have been used as secondary reference probes. In order to overcome the water solubility problems a more efficient water-soluble betaine dye (47) is produced by replacing some of the peripheral hydrophobic phenyl groups of the original betaine dye by more hydrophilic pyridyl groups. The excellent linear correlation between the  $E_T$  values of these dyes allow the calculation of  $E_T(30)$  values for solvents in which the solvatochromic indicator dye (44) is not soluble<sup>128</sup>.

$E_T(30)$  values cannot be measured for acidic solvents such as carboxylic acids because traces of an acid to solutions of the betaine dyes immediately changes its color to pale yellow due to protonation at the phenolic oxygen atom of the dye. The protonated form doesn't exhibit the long wavelength solvatochromic absorption band. The excellent linear correlation between  $E_T(30)$  and Kosower's  $Z$  values, which are available for acidic solvents, allows the calculation of  $E_T(30)$  values for such solvents<sup>128</sup>. Moreover, it is not possible to measure the absorption maximum of the standard betaine dye (44) in the gas phase as a reference state.

### 3.3.6. Multiparameter approaches to solvent polarity

There are many examples of solvent-sensitive processes which cannot be correlated by a single empirical solvent parameter. It has been told that the solvation power of a solvent is due to various nonspecific and specific solute-solvent interactions which are the result of many different

kinds of interaction mechanisms between the molecules of the solute and the solvent. So, the expression of solvent polarity as a single, universally determinable and applicable solvent parameter is an oversimplification. The separation of solvent polarity into various solute-solvent interaction mechanisms is useful because then the resultant parameters could be used to interpret solvent effects through such multiple correlations and provide information about the type and magnitude of interactions with the solvent. In such a case, only applications to processes that have the same relative sensitivity to various interaction mechanisms as the single solvent parameter will give a good correlation. However, such a separation is purely formal and may not be even theoretically valid as the interactions could be coupled and not operate independently of each other<sup>128, 136</sup>.

There have been many such multiparameter approaches to explain solvent effects on chemical and physical properties of solutes<sup>136</sup>. Katritzky was the pioneer in the establishment of multiparameter approaches to solvent polarity<sup>144</sup>. He tested various multiparameter equations using linear combinations of existing empirical solvent parameters with functions of the dielectric constant and index of refraction and was able to construct a two-parameter equation that allows independent variation of dipole/dipole and hydrogen-bonding forces.

The common expressions of multiparameter approaches take the form of linear free energy relationships (LFER)<sup>136, 145, 146</sup>. LFERs are not a necessary consequence of thermodynamics but still occur widely and provide information not otherwise accessible. Hence, the functional relationships between solvent parameters and various solvent-dependent processes often take the form of LFERs. Koppel – Palm multiparameter equation was the first popular LFER which use four parameters for characterizing solvents: polarity (Y), polarizability (P), electrophilicity/acidity (E), and nucleophilicity/basicity (B)<sup>136, 146</sup>. The expression, as shown in equation 3.17, also includes regression coefficients y, p, e and b which represent the susceptibilities of the solvent sensitive process to the influences of solvent polarity and polarizability, electrophilicity and nucleophilicity.

$$A = A_0 + yY + pP + eE + bB \quad (3.17),$$

where A is the solvent-sensitive characteristic for a given process and A<sub>0</sub> is equal to the A value, for the gas phase.

However, the more general approach was made by the group of Kamlet and Taft<sup>147-153</sup>. They assumed that attractive solute-solvent interactions are frequently of two kinds: nonspecific dipolarity/polarizability and specific hydrogen-bond complex formation. The second kind is subdivided into solute HBD/solvent HBA complex formation and solute HBA/solvent HBD complex formation. It was further assumed that the linear free energy relationships holds true for each of the contributing terms to the observed solvent effects. They have introduced the term linear solvation energy relationship (LSER) for generalized treatment of solvation effects. Frequently the following three “solvatochromic parameters” have been used in their studies to describe the solute and solvent properties.

- i. The  $\pi^*$  parameter is a measure of solute or solvent dipolarity/polarizability which estimates the ability of the solvent to stabilize a charge or a dipole by virtue of its dielectric effect. It was selected to run from 0.0 for cyclohexane to 1.0 for dimethyl sulfoxide.
- ii. The  $\alpha$  parameter represents the HBD acidities which applies to self-associating compounds when they act as solvents. It describes the ability of a solvent to donate a proton in a solvent-to-solute hydrogen bond. This parameter was selected to extend from 0.0 for non-hydrogen-bond donor solvents to ~1.0 for methanol.
- iii.  $\beta$  is the parameter for HBA basicities which applies to self-associating compounds when they act as solvents. It describes the solvent’s ability to accept a proton or donate an electron pair in a solute-to-solvent hydrogen bond. It was chosen to vary from 0.0 for non-hydrogen-bond donor solvents to ~1.0 for hexamethylphosphoric acid triamide (HMPT).

The parameters  $\alpha$  and  $\beta$  are replaced by  $\alpha_m$  and  $\beta_m$  when self-associating compounds are acting as “monomeric” solutes. Occasionally some other terms are used too, e.g. a discontinuous “polarizability correction term” ( $\delta$ ), an amphiprotic hydrogen-bonding parameter ( $\omega$ ), the Hildebrand solubility parameter ( $\delta_H$ ), a coordinate covalency parameter ( $\xi$ ) etc.

The solvatochromic parameters are reported for a large number of solvents. These were calculated by averaging the multiple normalized solvent effects on a variety of solvent-dependent properties involving various types of solvatochromic indicator dyes. Therefore, these solvatochromic parameters are no longer directly based on the solvent effects indicated by a

distinct single solvatochromic indicator dye. Rather, they are statistically averaged values resulting from a series of successive approximations. Kamlet and Taft's solvatochromic parameters have been used in different combinations in one-, two-, and three-parameter correlations. In the common representation of solvatochromic comparison method, the solvent dependent property  $A$  is expressed as a function of  $\pi^*$ ,  $\alpha$  and  $\beta$  [equation 3.18].

$$A = A_0 + s\pi^* + a\alpha + b\beta \quad (3.18).$$

If the spectral maximum is chosen as the solvent dependent property then equation 3.18 becomes equation 3.19.

$$\sigma = \sigma_0 + s\pi^* + a\alpha + b\beta \quad (3.19).$$

The solvatochromic comparison method fails to accurately describe the solvatochromic behavior of nonpolar solutes exhibiting no specific interaction with the solvent. The  $\pi^*$  parameter reflects a mixed effect of solvent dipolarity and polarizability and hence cannot describe a solvatochromic behavior exclusively predicted in terms of changes in solvent polarizability. Catalan developed a general, multiparameter scale for describing the solvent polarity based on two specific scales: solvent acidity (SA) and basicity (SB); and two general scales: solvent polarizability (SP) and dipolarity (SdP)<sup>128, 154</sup>. This SP and SdP parameters are actually contained in the Kamlet and Taft's  $\pi^*$  parameter. Catalan's scheme was formulated as follows [equation 3.20]:

$$\sigma = \sigma_0 + bSA + cSB + dSP + eSdP \quad (3.20).$$

Here SA, SB, SP, and SdP represent independent but complementary solvent parameters which accounts for various types of solute - solvent interactions; and b to e are the regression coefficients describing the sensitivity of property  $A$  to the different solute - solvent interaction mechanisms. Catalan's approach allows one to accurately describe the solvent effect experienced by any solutes whether polar or nonpolar and exhibiting some or no specific interaction with the solvent.

### 3.3.7. Effect of temperature and viscosity on fluorescence spectra

Increase in temperature and decrease in viscosity or vice versa poses significant influence on the fluorescence spectra<sup>7, 30</sup>. Frequency of molecular collision increases with increase in temperature

and decrease in viscosity and as a result the nonradiative processes prevail and fluorescence yield decreases. There is also another type of influence. The rate of solvent relaxation is normally much faster than the fluorescence decay rate in fluid solvents and so the emission spectrum reveals the relaxed state. If the temperature is decreased and viscosity is increased to the extent when two rates become similar, then emission and relaxation will occur simultaneously and an intermediate emission spectrum will be observed. Frequently this intermediate spectrum is broader on the wavelength scale because of contributions from both the Frank-Condon and relaxed states. If the temperature is further lowered or the viscosity increased, then fluorescence emission will occur before solvent relaxation and is indicative of the Frank-Condon state.

### 3.3.8. Fluorescence in mixed solvent systems and preferential solvation

Binary solvent mixtures often have an enhanced ability to dissolve certain substances, and therefore, used frequently in many industrial processes as well as laboratory procedures. The solvent mixtures usually have improved physical properties, such as the density, viscosity, volatility etc. as well as chemical properties, such as stability, inflammability etc. A combination of all these facts makes binary solvent mixtures an important media for scientific investigation

155-158

Spectral maxima or quantum yields of polarity sensitivity of fluorophores vary according to the nature of the solvent or the type of the binding site in macromolecules. Usually the unknown polarity of the probe binding site on the macromolecule is determined by comparison of the emission maxima and/or quantum yields (observable) when the fluorophore is bound to the macromolecule or dissolved in solvents of different polarity. A calibration curve of the observable vs.  $E_T(30)$  is prepared for the accurate determination of binding site polarity. In practice, however, different compositions of the solvent mixture of water and 1,4-dioxane is used in preference to solvents of different polarity. The properties of the binary solvent mixture of water and 1,4-dioxane is thoroughly investigated and reported in literature<sup>159-161</sup>. The reason for the preference is to avoid the inclusion of different solvent specific interactions into calibration curve. It is, however, worthy to mention that such a replacement is feasible only if the photophysics of the fluorophore in mixed solvent systems is quite similar to that in homogeneous solvents.

The solubility of solutes in a mixed solvent system depends primarily on the solvation of solutes by the components of the solvent mixture. The scenario is, however, more complex, because a solvent mixture involves interactions not only between the solute and solvent but also among different molecules present in the mixture; the latter type of contribution also plays a central role in the solvation process. Depending on its nature, the solute may induce a change with respect to the bulk solvent in its environment so that the proportion of solvent components may be significantly different around the solute and in the bulk solution. This phenomenon is known as preferential solvation and it leads to a more negative Gibbs energy of solvation<sup>161-165</sup>. Such a change takes place via either non-specific solute-solvent interactions called dielectric enrichment or specific solute-solvent association (e.g. hydrogen bonding).

The theory of dielectric enrichment was developed by Suppan *et.al.*<sup>129</sup> and has been extensively explored in several literature reports. This model is based on the Onsager description of electrostatic solute - solvent interactions, and hence considers a mixed solvent system as an ideal mixture of continuous dielectric solvents without any specific interactions. For a mixture of polar and nonpolar solvents, suppose  $x_n$  and  $x_p$  are the bulk mole fractions of the nonpolar and polar components respectively. Similarly, suppose  $y_n$  and  $y_p$  are the local mole fractions of the nonpolar and polar components respectively. According to Suppan, the local composition in the near vicinity of a dipolar solute is given by equation 3.21<sup>166</sup>,

$$\frac{y_n}{y_p} = \frac{x_n}{x_p} e^{-Z} \quad (3.21),$$

where,  $Z$  is referred as the index of preferential solvation.

It is worth reiterating that the process of dielectric enrichment does not account for any specific solute – solvent interactions such as hydrogen bonding. Therefore, equation 3.21 is not suitable for specific associations and actually the deviations can be used to distinguish between specific and nonspecific interactions. This procedure is occasionally used to compare fluorescence Stokes shift of dipolar solutes in mixed solvents, such as toluene – acetonitrile and toluene – methanol mixtures. Considering pure electrostatic solute – solvent interactions, the solvation ability of any solvent can be expressed by the reaction field factor  $F(\epsilon, n)$ . The reaction field factor is often used

as a measure of the solvation energy. It is a function of the dielectric constants  $\epsilon$  and refractive indexes  $n$  [equation 3.22] <sup>166</sup>.

$$F(\epsilon, n) = \frac{\epsilon - 1}{\epsilon + 2} - \frac{n^2 - 1}{n^2 + 2} \quad (3.22).$$

Acetonitrile and methanol have similar dielectric constant and refractive index and hence both offer the same solvation ability. Therefore, toluene – acetonitrile and toluene – methanol mixtures should behave identically. However, methanol is capable of forming hydrogen bonds with appropriate solutes and as a consequence, deviations from equation 3.21 is observed <sup>166-169</sup>.

It is essential to mention that the dielectric constant  $\epsilon$  and refractive index  $n$  of a solvent mixture are obtained by fitting the experimental data. For toluene-acetonitrile and toluene-methanol solvent mixtures, Krolicki *et.al.* have reported the following empirical equations 3.23, 3.24, 3.25 and 3.26 <sup>169</sup>:

For toluene – acetonitrile solvent mixture

$$n = 1.495 - 0.084x_p + 0.003x_p^2 - 0.072x_p^3 \quad (3.23),$$

$$\epsilon = 2.38 + 14.6x_p - 4.16x_p^2 + 22.9x_p^3 \quad (3.24).$$

For toluene – methanol solvent mixture

$$n = 1.495 - 0.063x_p + 0.014x_p^2 - 0.117x_p^3 \quad (3.25),$$

$$\epsilon = 2.38 + 6.13x_p + 0.14x_p^2 + 24.03x_p^3 \quad (3.26).$$

### 3.4. Fluorescence Quenching

Fluorescence quenching is a general term that refers to any process that reduces the fluorescence intensity of sample, without any permanent change in the molecules. Broadly, there are two kinds of quenching: static and dynamic <sup>7, 30</sup>. Static quenching arises from any process that lowers the population of electronically excited fluorophore, especially by forming a ground state nonfluorescent complex. Dynamic quenching happens from any process that affects the fluorophore in its excited state, such as energy transfer, PET, PPT etc. <sup>170-172</sup>.

Fluorescence quenching is widely studied as a source of information about biochemical systems. Most processes leading to quenching requires molecular contact between the fluorophore and the

quencher, and hence, quenching measurements can reveal the accessibility of fluorophores to quenchers. In addition, the diffusion constant of the quencher can be measured from the rate of collisional quenching.

In absence of static quenching, the dynamic quenching of fluorescence can be described by the Stern-Volmer equation [equation 3.27] <sup>173</sup>:

$$\frac{F_0}{F} = 1 + k_q \tau_0 [Q] = 1 + K_D [Q] \quad (3.27),$$

where,  $F_0$  and  $F$  are the fluorescence intensities in the absence or presence of quencher, respectively;  $k_q$  is the bimolecular quenching constant;  $\tau_0$  is the lifetime of the fluorophore in the absence of quencher, and  $Q$  is the quencher concentration. The Stern-Volmer dynamic quenching constant is given by  $K_D = k_q \tau_0$  <sup>7</sup>.

Quenching data are usually presented as plots of  $F_0/F$  versus  $[Q]$ , which gives linear fit with an intercept of one on the y-axis and a slope equal to  $K_D$ . Stern-Volmer Plot will display downward curvature when the gross fluorescence is due to multiple fluorophores differently accessible to quenchers <sup>174</sup>.

In many instances, static quenching occurs simultaneously with dynamic quenching, and the Stern-Volmer plots in such circumstances show an upward curvature, concave towards the y-axis. In such cases, the fractional fluorescence  $F_0/F$  is given by the modified form of the Stern-Volmer equation [equation 3.28] <sup>7, 30</sup>.

$$\frac{F_0}{F} = (1 + K_D [Q])(1 + K_S [Q]) \quad (3.28).$$

In some cases, an apparent static component may arise due to the quencher being adjacent to the fluorophore at the instant of photoexcitation. Due to these close association, such fluorophore-quencher pairs are immediately quenched, and thus appear to be dark complexes. This type of apparent static quenching is usually interpreted in terms of a sphere of action within which the probability of quenching is unity. Following modified version of Stern-Volmer equation describes such situation [equation 3.29] <sup>7, 175, 176</sup>:

$$\frac{F_0}{F} = (1 + K_D[Q]) \exp\left(\frac{[Q]VN}{1000}\right) \quad (3.29),$$

where V is the volume of the sphere.

### 3.5. Excitation energy transfer

The electronic excitation energy of a molecule can be dissipated by transferring it to another molecule that is chemically different (heterotransfer) or identical (homotransfer)<sup>30</sup>. The energy transfer can take place via radiative or nonradiative pathway<sup>30, 177-179</sup>. In radiative transfer pathway, the photon emitted by the donor molecule is absorbed by the acceptor molecule when the average distance between the two is larger than the wavelength. In contrast, nonradiative transfer occurs without emission of photons at distances less than the wavelength and results from short- or long-range interactions between the molecules. For both types of energy transfer, it is necessary to have spectral overlap between the emission spectrum of the donor and the absorption spectrum of the acceptor. Apart from that, the factors governing the efficiency of radiative and nonradiative transfers are not the same.

Radiative and nonradiative transfers have different effects on the characteristics of fluorescence emission from the donor<sup>30</sup>. Radiative energy transfer modifies the fluorescence spectrum of the donor due to quenching of the fluorescence intensity in the region of spectral overlap. Such a distortion of the fluorescence spectrum is called the secondary or emission inner filter effect. In case of nonradiative energy transfer, the fluorescence intensity of the donor is quenched by the same factor throughout the spectrum. Fluorescence decay patterns reveal further differences between the two kinds of energy transfer. In the case of radiative transfer between identical molecules, the fluorescence of the donor decays more slowly as a result of successive re-absorptions and re-emissions. However, homotransfer via nonradiative pathway does not affect the fluorescence decay time of the donor. In contrast, heterotransfer via radiative pathway keeps the fluorescence decay time unchanged, although it gets shortened in the case of nonradiative transfer.

Nonradiative transfer takes place if several vibronic transitions in the donor have practically the same energy as the corresponding transitions in the acceptor in the region of spectral overlap. In this way the transitions are coupled, i.e. are in resonance and hence the term resonance energy

transfer (RET) is often used. Another acronym FRET is also used, denoting fluorescence resonance energy transfer, but it is recommended to use RET because it is not the fluorescence that is transferred but the electronic energy of the donor, and that non-fluorophores can also participate in RET process<sup>30</sup>.

Four factors generally contribute towards the rate or efficiency of RET process<sup>177-179</sup>.

1. The extent of spectral overlap of the emission spectrum of the donor with the absorption spectrum of the acceptor.
2. The donor-to-acceptor distance.
3. Relative orientations of the transition dipoles of the donor and acceptor.
4. The quantum yield of the donor.

RET can result from different interaction mechanisms which may be Coulombic and/or due to intermolecular orbital overlap<sup>30,177-179</sup>. The Coulombic interactions consist of long-range dipole-dipole and short-range multi-polar interactions, whereas the interactions due to intermolecular orbital overlap are only short range including electron exchange and charge resonance interactions. In some RET process, the initially excited electron on the donor returns to the ground state orbital of the donor, while simultaneously an electron on the acceptor is promoted to the excited state. This process is possible only for allowed transitions on the donor and the acceptor and is predominantly triggered by the Coulombic interaction, even at short distances. For forbidden transitions on the donor and the acceptor, RET is associated with an exchange of two electrons between donor and acceptor. Coulombic interaction has negligible contribution on such RET process, which is mainly guided by short-range interactions due to intermolecular orbital overlap.

The rate of RET  $k_T(r)$  at  $r$  distance between the donor and acceptor is given by equation 3.30<sup>180</sup>,

$$k_T(r) = \frac{1}{\tau_D} \left( \frac{R_0}{r} \right)^6 \quad (3.30),$$

where  $\tau_D$  is the decay time of the donor in the absence of acceptor,  $R_0$  is the D–A distance at 50% transfer efficiency, known as the Förster distance.

The efficiency of energy transfer was determined from the equation 3.31:

$$E = 1 - \left( \frac{F}{F_0} \right) = \frac{R_0^6}{(R_0^6 + r^6)} \quad (3.31),$$

$R_0$  is calculated using equation 3.32:

$$R_0^6 = 8.79 \times 10^{-25} \kappa^2 \eta^{-4} J(\lambda) \Phi \quad (3.32),$$

The value of  $J(\lambda)$  has been calculated using equation 3.33:

$$J(\lambda) = \frac{\int F_D(\lambda) \varepsilon_A(\lambda) \lambda^4 d\lambda}{\int F_D(\lambda) d\lambda} \quad (3.33),$$

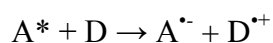
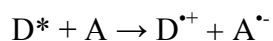
$F_D(\lambda)$  is the fluorescence intensity of HSA (donor) at wavelength  $\lambda$  and  $\varepsilon_A(\lambda)$  is the molar extinction coefficient of BINOL at the same wavelength.  $\Phi$  is the quantum yield of the donor HSA.  $\eta$  is the refractive index of the medium.  $\kappa$  is the orientation factor of the donor and acceptor and for random orientation of donor and acceptor a value of  $2/3$  is assumed for  $\kappa^2$ .

The rate of RET depends strongly on D–A distance and is proportional to  $r^{-6}$ , and thus, RET measurement is often described as a “spectroscopic ruler”<sup>30</sup>. It is frequently used to measure the donor-to-acceptor distance between two sites of a macromolecule, usually when the Förster distance ranges from 20 to 90 Å<sup>26, 27, 34, 41, 42</sup>. For example, RET can be used to measure the distance from a tryptophan residue to a ligand binding site when the ligand acts as an acceptor and the tryptophan as a donor. Often, in larger assemblies of macromolecules, there is more than a single acceptor near a donor molecule. Such systems can also be studied by RET. Even with a single D–A pair, there can be more than a single D–A distance by the presence of donor to acceptor diffusion during the donor lifetime<sup>7</sup>. Such instances are in membranes where the acceptor is a freely diffusing lipid analogue, or in unfolded proteins, where the drug-tryptophan or drug-tyrosine distances are variable. If the D–A distance remains the same during the excited state lifetime of the donor, then the RET efficiency can easily be calculated from steady-state fluorescence measurements. If the presence of donor-to-acceptor diffusion affects the D–A distance during the donor lifetime, time-resolved techniques are usually used for obtaining the details. RET is also used in studies in which the actual D–A distance is not being measured<sup>7</sup>. The binding interaction of two macromolecules that are individually labeled with donor or

acceptor can be measured using RET. Typical experiments of this type include DNA hybridization or any bioaffinity reactions.

### 3.6. Photoinduced electron transfer

An electronically excited molecule has an increased tendency to give away or accept an electron, due to alteration of electron density on photoexcitation, and therefore, absorption of a photon activates molecules to undergo redox reactions or photo induced electron transfer (PET) <sup>30, 181-186</sup>. In PET, the species that donates an electron and gets oxidized is referred to as a donor (D), and an acceptor (A) is a species that gets reduced by accepting an electron. The fluorophore can either be a donor or an acceptor, determined by its oxidation and reduction potential in the ground and excited states. Often, in such reactions, the fluorophore is termed as the sensitizer and the other molecule as the quencher. The oxidative and reductive electron transfer processes can be represented as follows,



where,  $D^{\bullet+}$  and  $A^{\bullet-}$  are the transient radical cation and anion, respectively. The transferred electron in PET reactions, in principle, can go back to the donor in a process known as back electron transfer (BET) <sup>18, 183</sup>. BET is an energy wasting process as it regenerates the donor and acceptor molecules in their ground states.

In nature, PET is used as a mode of molecular activation in photosynthetic reaction center in order to convert solar energy to chemical energy via charge transfer <sup>30</sup>. Here, the antenna chromophores absorb light, which initiates a series of PET. Such cascades of donor and acceptor substrates in the photosynthetic system prevent BET processes.

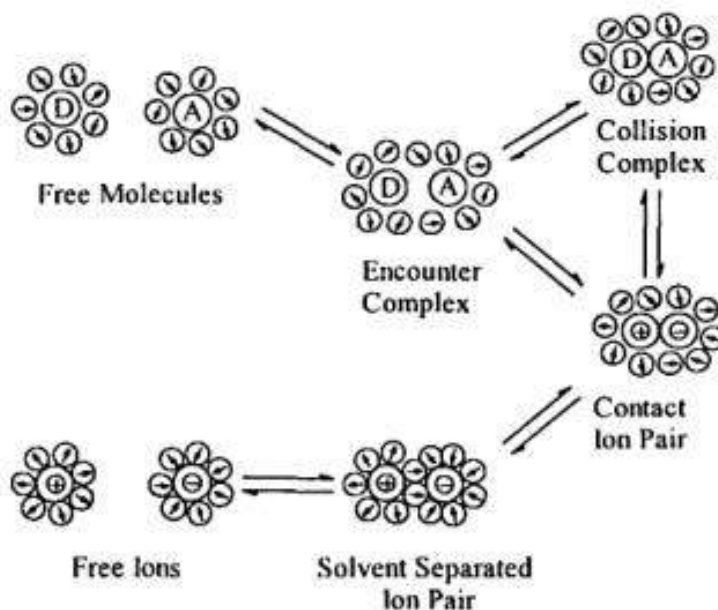


**Figure 3.2.** Schematic diagram summarizing the various events in PET reaction <sup>183</sup>.

For electron transfer reaction in solution, the reactants are free to move around, and the interaction between the sensitizer and the quencher creates a series of short-lived intermediates, each possessing a unique geometry and electronic distribution <sup>18, 183</sup>. The donor and the acceptor can diffuse towards each other by a series of one-dimensional random steps leading to the formation of an encounter complex. Further diffusion results in the formation of the collision complex, which can be visualized as an ensemble surrounded by several layers of solvent molecules. Electron transfer can take place either within the collision complex or the encounter complex, and as a consequence, contact ion pair (CIP) is formed, followed by the solvent separated ion pair (SSIP). In SSIP, the opposite ions are separated by one or two solvent molecules. Occasionally, the CIP and SSIP are referred to as the geminate ion pairs. Finally, the ions move apart to form free solvated ions. The efficiency of a PET reaction depends on the yield of free ions, because BET is facile with CIP or SSIP. Figure 3.2 is a schematic diagram summarizing the various events in PET reactions.

Quenching of the sensitizer fluorescence is a consequence of PET reactions but a more definitive study is carried out with the help of laser flash photolysis, a special type of pump-probe spectroscopy <sup>184-186</sup>. In this technique, a short pulse of laser radiation is used to interact with a

sample that has been placed in the optical path of a spectrometer. Consequently, the absorbance of the transient radical ions, resulting from PET reactions, at a particular wavelength or range of wavelengths, is recorded as a function of time<sup>187, 188</sup>. The time-resolved transient absorbance spectrum is constructed by plotting the transient absorbance values at a particular time delay versus the wavelengths.

### 3.7. Photoinduced proton transfer

The acidic or basic properties of a chromophore may not be the same in the ground state and in the excited state, and this happens due to the redistribution of the electron density upon excitation. Such differences can be revealed by comparing the changes in the absorption and fluorescence spectra of a fluorophore at different pH. To observe any difference, however, the acid-base reaction has to take place in a time period less than the lifetime of the photoexcited state<sup>4, 30</sup>. The Brønsted acid-base reaction, which involve transfer of protons usually take place faster than the fluorescence decay. 1-naphthylamine-4-sulphonate and 3-hydroxypyrene-5,8,10-trisulphonate are examples of these kind of fluorophores. In these cases, the acids are stronger than in the ground state and photoexcitation triggers a photoinduced proton transfer (PPT). Then, the acidic character of the proton donor group ( $-\text{NH}_2$  or  $-\text{OH}$ ) is enhanced on photoexcitation so that the  $\text{pK}^*$  of this group in the excited state is much lower than in the ground state. In the same way, the  $\text{pK}^*$  of the proton acceptor group in a fluorophore is higher in the excited state than in the ground state ( $\text{pK}$ ).

The excited state proton transfer (ESPT) decreases the population of the fluorophore and increases the population of the deprotonated/protonated species, which also remains in the photoexcited state<sup>189</sup>. The deprotonated/protonated species is generally lower in energy than the parent fluorophore and deexcites via partially radiative or completely nonradiative pathway.

### 3.8. Fluorescence polarization spectroscopy

It has already been mentioned that light is an electromagnetic wave consisting of an electric field and a magnetic field perpendicular to each other and to the direction of propagation and oscillating in phase<sup>2</sup>. For normal light, these fields have no preferential orientation but for linearly polarized light, the electric field oscillates along a given direction, the intermediate case

corresponds to the partially polarized light. A fluorophore preferentially absorbs photons whose electric field vectors are aligned parallel to the transition dipole moment of the fluorophore. Thus, when a randomly oriented population of fluorophore in an isotropic solution is illuminated by a linearly polarized beam of incident light, those, whose transition moments are oriented in a direction close to the electric field of the incident beam, are excited in preference to others. This phenomenon is called photoselection which results in an anisotropic distribution of excited fluorophores with subsequent emission of partially polarized or anisotropic fluorescence<sup>7,30</sup>.

To measure the fluorescence anisotropy, the sample is excited with vertically polarized light and the intensity of the emission is measured through a polarizer. When the emission polarizer is oriented parallel ( $\parallel$ ) to the direction of the polarized excitation the observed intensity is denoted as  $I_{\parallel}$ . Likewise, when the polarizer is perpendicular ( $\perp$ ) to the excitation the intensity is denoted as  $I_{\perp}$ . Hence, the anisotropy ( $r$ ) is given by equation 3.34.

$$r = \frac{I_{\parallel} - I_{\perp}}{I_{\parallel} + 2I_{\perp}} \quad (3.34).$$

Fluorescence anisotropy is a dimensionless quantity that is independent of the total intensity of the sample and also of the fluorophore concentration in absence of artifacts.

If the direction of the transition moment changes during the excited state lifetime of the fluorophore, its fluorescence anisotropy will decrease with partial or complete depolarization of fluorescence. The transition dipole moment of an excited fluorophore may change for various reasons: rotational diffusion, torsional vibration, non-parallel absorption and emission transition moments and transfer of excitation energy to another molecule with different orientation of the transition moment<sup>30</sup>. Fluorophores in non-viscous solution can rotate many times during the excited state lifetime, causing the polarized emission to randomize and therefore, near zero fluorescence anisotropies are displayed. Binding to an inhomogeneous medium slows down the rotational diffusion of the fluorophore. In absence of other anisotropy-influencing processes, the expected anisotropy is given by the Perrin equation [equation 3.35].

$$r = \frac{r_0}{1 + (\tau / \theta)} \quad (3.35),$$

where,  $r_0$  is the anisotropy that would be measured in the absence of rotational diffusion, and  $\theta$  is the rotational correlation time for the diffusion process. It is evident that the measurements of fluorescence anisotropy will be sensitive to any factor that affects the rate of rotational diffusion. Fluorescence anisotropy measurements provide valuable information on molecular mobility, flexibility, size and shape, fluidity of a medium etc.<sup>32,34</sup>.

### 3.9. Red-edge-excitation fluorescence spectroscopy

If a fluorophore is dissolved in a motionally restrained media, the solvent relaxation may take place on the nanosecond time scale. Thus, fluorescence emission occurs to a considerable extent during solvent relaxation. As a consequence, the fluorescence spectrum represents a time-average of the emissions from different partially relaxed states. In such a scenario, the emission maximum no longer remains correlated with solvent polarity. Increase in temperature fastens solvent reorientation, and therefore, leads to a red shift of the emission maxima. The more interesting observation, however, is the excitation wavelength dependence of emission spectra. Such a shift in the wavelength of fluorescence maximum towards higher wavelengths, caused by a shift in the excitation wavelength towards the red edge of absorption band, is termed red edge excitation shift (REES)<sup>7</sup>. REES is mostly observed with polar fluorophores in highly viscous solutions or condensed phases or when the fluorophore binds/partitions to a constrained media such as micelles, reverse micelles, proteins, nucleic acids etc.<sup>190-194</sup>. REES is maximal when the solvent relaxation is much slower than fluorescence, and it should be zero if the relaxation process is fast enough. Depending on the chosen solute-solvent system, the REES value can range from several upto 40 nm. Measurements of REES, makes it possible to probe the mobility parameters of the probe's environment using the probe merely as a reporter molecule. It is the only steady-state measurement that provides information about the relative rates of solvent relaxation dynamics.

### 3.10. Synchronous fluorescence spectroscopy

For a mixture of fluorescent compounds dissolved in a solvent, usually the analysis is done by excitation at various fixed wavelengths selected specifically for individual components. However, for complex multi-component mixtures, such procedure does not give satisfactory results, because of the severely overlapping emission and/or excitation spectra. In such cases,

considerable improvement can be made when excitation and emission wavelengths are varied together by scanning both the monochromators simultaneously. This process is known as synchronous fluorescence spectroscopy (SFS)<sup>195-201</sup>. Here, the fluorescence contributed by each component is restricted to that excited at wavelengths synchronously trailing the plotted emission. The selectivity of SFS can still be increased by taking derivative spectrum, applying different multivariate methods, selective fluorescence quenching, three-dimensional synchronous measurement or using some of these procedures in combination. Lloyd introduced this technique in 1971<sup>195</sup>. Subsequently, Vo-Dinh formulated the basic theory and suggested experimental procedures to allow measurement of spectral signatures from complex samples, and other specific information of analytical interest<sup>196, 197</sup>. Today SFS is successfully being used by forensic researchers, oil-spill analysts, analytical chemists and also in a few biophysical studies<sup>197-201</sup>. For instance, contribution of tryptophan and tyrosine towards protein fluorescence can be evaluated by using offsets of 60 nm and 15 nm, respectively.

In the common mode of SFS, the scan rate is kept constant for both the monochromators, and therefore, a constant wavelength interval,  $\Delta\lambda$ , known as the offset, is maintained between the excitation and emission wavelengths. This simple technique is known as constant-wavelength SFS and is the most frequently used of all synchronous modes. A signal is observed only when  $\Delta\lambda$  matches the interval between one absorption band and one emission band. The most intense synchronous signal with narrowest half-width is achieved when  $\Delta\lambda$  is chosen to match the wavelength interval between the maxima of these two peaks.

There are three main characteristics of SFS which highlight its usefulness<sup>83,87</sup>:

1. Emission spectrum of a complex mixture is diffuse because the emission bands of each individual spectrum are intrinsically broad. Moreover, the various spectra overlap severely causing further diffuseness. The synchronous spectrum has narrow spectral bands as a consequence of the multiplication of two functions increasing and/or decreasing simultaneously.
2. In multicomponent mixtures, synchronous scan with the use of a suitable offset makes the spectra considerably simplified by allowing the stronger peaks to be increased, and reducing the interferences resulting from spectral superposition. It is thus possible to analyze selectively a certain component in such mixture with high precision.

3. From an analytical viewpoint, one or several spectral bands are useful, not the detailed structure of the entire emission spectrum. Presence of the most other spectrometric details serves only to confuse the total spectrum by interfering with the emission of other components in the mixture. Synchronous scan modifies the spectral band width of the emission signal of each individual component in a mixture and thereby eliminates the unnecessary details from the emission spectra.

### 3.11. Time-correlated single-photon counting

The time-resolved measurements of fluorescence contain more information than is available from the steady-state data. Usually fluorescence lifetimes and anisotropies are measured in this way. There are two dominant methods for time-resolved measurements: the time-domain and frequency-domain methods. From the last decade, due to the advancement of newer technologies, the time-domain method has become smaller, less expensive, and more reliable. In the recent literatures, time-domain fluorescence measurements using time-correlated single-photon counting (TCSPC) appears frequently<sup>202-204</sup>.

In the time-domain methods of measuring time resolved fluorescence, the sample is excited with a short pulse of light, and thereafter the intensity decay is measured through a polarizer oriented at magic angle from the vertical z-axis. The decay time of the sample is calculated from the slope of  $\log I(t)$  vs.  $t$ . The width of the excitation pulse is kept much shorter than the decay time  $\tau$  of the sample. The magic angle condition is used to eliminate the artifacts resulting from rotational diffusion and/or anisotropy on the intensity decay. The magic angle, which is a root of a second order Legendre polynomial,  $P_2(\cos \theta) = 0$ , is a precisely defined angle with an approximate value of  $54.7356^\circ$ .

In TCSPC, the sample is excited with a pulse of light, but conditions are adjusted so that less than one photon is detected per laser pulse, typically 1 photon per 100 excitation pulses. Even if multiple photons are produced per pulse, TCSPC allows detecting only the first photon. The probability of detecting the single photon at time  $t$  after an exciting pulse is proportional to the fluorescence intensity at that time.

### 3.12. Ligand binding studies from fluorescence

Emission spectra are easily measured, resulting in numerous publications on emission spectra of fluorophores in different solvents, and when bound to macromolecules like proteins, membranes etc. Such results are needed to determine the polarity of the probe binding site on the macromolecule by comparison of the emission spectra and/or quantum yields when the fluorophore is bound to the macromolecule or dissolved in solvents of different polarity. Moreover, binding of a fluorophore to a macromolecule causes a spectral shift or change in quantum yield of the fluorophore emission. Alternatively, the ligand may induce a spectral shift in the intrinsic or extrinsic fluorescence of the macromolecule. In either case the spectral changes can be used to measure the extent of binding. Absorption spectra have similar uses if solvent perturbation is significant.

For a host–guest molecular complexation reaction, suppose that the guest concentration is being increased stepwise in the system containing a fixed concentration of the host, until the guest concentration becomes much larger than the initial concentration of the host. Supposing that the host fluorescence changes by  $\Delta F$  at an intermediate concentration of the guest and by  $\Delta F_{\max}$  at the maximum concentration of the host, the equilibration is described according to the Benesi-Hildebrand double reciprocal equation<sup>205-212</sup> [equation 3.36].

$$\frac{1}{\Delta F} = \frac{1}{\Delta F_{\max}} + \frac{1}{\Delta F_{\max}} \left( \frac{1}{K[L]} \right) \quad (3.36),$$

where,  $K$  is the binding constant, and  $[L]$  is the total protein concentration. The rearranged version of the Benesi-Hildebrand equation is used to find the binding constant  $K$  by plotting  $(\Delta F_{\max}/\Delta F) - 1$  against  $[L]^{-1}$  [equation 3.37].

$$\frac{\Delta F_{\max}}{\Delta F} - 1 = \frac{1}{K[L]} \quad (3.37),$$

Benesi-Hildebrand will give excellent linear plots for 1:1 complex formation. For other complex formation stoichiometry, this method may generate inappropriate parameters that significantly interfere with the accurate determination of association constants. So, Scatchard plot has become the most common presentation of ligand- acceptor binding data in the biological sciences<sup>213-221</sup>.

The Scatchard equation is given by equation 3.38:

$$\frac{r}{c} = nK - rK \quad (3.38),$$

where,  $r$  represents the number of guest molecules bound to one host molecule,  $c$  is the unbound guest concentration,  $n$  is the number of independent binding sites on one host molecule, and  $K$  is the binding constant. The plot of  $(r/c)$  versus  $r$  is linear if the binding is independent to sites of the same affinity. The binding constant as well as the number of independent binding site is obtained from the slope and the intercept of the linear plot. A nonlinear Scatchard plot can represent two classes of binding sites: independent or dependent. In such cases an appropriate computer program, such as “LIGAND”, is recommended to use for extraction of binding parameters from binding data<sup>220</sup>.

It is possible to find out the thermodynamic parameters responsible for the binding equilibrium from the van't Hoff equation<sup>222-227</sup> [equation 3.39]:

$$\ln K = -\frac{\Delta H^0}{RT} + \frac{\Delta S^0}{R} \quad (3.39),$$

where,  $K$  is the binding constant at corresponding temperature  $T$ , and  $R$  is the gas constant. A plot of  $\ln K$  versus  $(1/T)$  at different temperatures yields the standard enthalpy change ( $\Delta H^0$ ) and standard entropy change ( $\Delta S^0$ ) on binding. The standard free energy change can be calculated from equation 3.40:

$$\Delta G^0 = \Delta H^0 - T\Delta S^0 \quad (3.40),$$

### 3.13. Circular dichroism spectroscopy

Circular dichroism (CD) is a property possessed by some molecules, essentially chiral, by which the absorption of light circularly polarized in one direction (right-handed) is different from the absorption of the light circularly polarized in the opposite direction (left handed). It is recorded as a secondary absorbance component by switching between left and right circularly polarized light, and measuring the resulting difference in absorbance. CD spectroscopy has a wide range of applications including the structural study of biomolecules (such as proteins, nucleic acids, glycosides, etc.), investigation of the charge-transfer reactions, geometric and electronic structure

prediction of chiral metal complexes by probing metal d→d transitions, structural studies of small chiral organic molecules (using vibrational circular dichroism) etc.<sup>228-245</sup>.

CD measurements are frequently employed in the investigation of protein structure<sup>230-241</sup>. In the far ultraviolet region of the spectrum (wavelengths between 180 and 260 nm), the CD signal of proteins reports on its secondary structure, owing to the presence of the asymmetric  $\alpha$ -carbon atoms on either side of the amide chromophore of the peptide bond. In the near ultraviolet region of the spectrum (wavelengths between 250 and 350 nm), the chromophores are the aromatic amino acids and disulphide bonds, and the CD is sensitive to the tertiary structure of the protein. Time-resolved CD measurement is also in common use for studying protein folding, denaturation or renaturation processes. Such study can be made in the far UV to investigate secondary structure formation or in the near UV to study the development of tertiary structure.

The CD data is commonly recorded as ellipticity  $[\theta]$  (degrees) versus wavelength. The data is usually normalized by scaling to molar concentrations of either the whole molecule or the repeating unit of a polymer. For far UV CD of proteins, the repeating unit is the peptide bond. The Mean Residue Weight ( $\mu$ ) for the peptide bond is calculated from equation 3.41:

$$\mu = \frac{M}{N-1} \quad (3.41),$$

where  $M$  is the molecular mass of the polypeptide chain (in Da), and  $N$  is the number of amino acids in the chain; the number of peptide bonds is  $(N-1)$ . For most proteins  $\mu$  is  $110 \pm 5$  Da.

The mean residue ellipticity at wavelength  $\lambda$  is given by equation 3.42:

$$[\theta]_{\text{mrw},\lambda} = \frac{\mu\theta_{\lambda}}{10dc} \quad (3.42),$$

where  $\theta_{\lambda}$  is the observed ellipticity (degrees) at wavelength  $\lambda$ ,  $d$  is the pathlength (cm), and  $c$  is the concentration (g/ml).

### 3.14. Theoretical molecular docking calculations

Automated molecular docking is widely used in structural molecular biology for prediction of biomolecular complexes in structure-activity analysis and in structure-based drug discovery<sup>246-253</sup>. The ligand–protein docking aims to predict the predominant binding mode(s) of a ligand with a protein of known three-dimensional structure. The emergence of this method has been facilitated by the dramatic growth in availability and power of computers, and the growing ease of access to small molecule and protein databases.

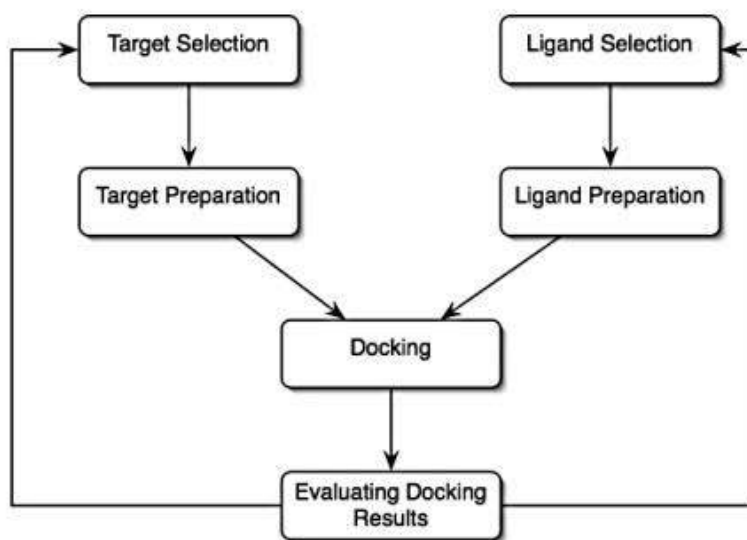


**Figure 3.3.** A typical docking workflow which shows the key steps common to all docking protocols<sup>246</sup>.

Dozens of effective methods are available to understand and predict molecular recognition, find the binding modes and predict the binding affinity. Figure 3.3 shows a typical docking workflow which shows the key steps common to all docking protocols. The success of any such methods depends on the effectiveness of the search in the high-dimensional spaces and the use of a scoring function to correctly rank the candidate dockings, with a reasonable computational effort. Comparing docking methods is difficult, and because there is evidence that some docking methods do better with certain classes of target than others. Hence, it is preferred to try several docking methods to determine which one(s) work best for the target of interest.